# TUDelft

Delft University of Technology

## Ramp sinusoidal breakdown of epoxy resin under high voltage waveforms at different frequencies

Zhao, W.; Luo, T.; Ghaffarian Niasar, M.

**Citation (APA)**
Zhao, W., Luo, T., & Ghaffarian Niasar, M. (2021). Ramp sinusoidal breakdown of epoxy resin under high voltage waveforms at different frequencies. In *22nd International Symposium on High Voltage Engineering (ISH 2021)* (15 ed., Vol. 2021, pp. 2083-2088) https://doi.org/10.1049/icp.2022.0291

**Important note**
To cite this publication, please use the final published version (if applicable).
Please check the document version above.

# RAMP SINUSOIDAL BREAKDOWN OF EPOXY RESIN UNDER HIGH VOLTAGE WAVEFORMS AT DIFFER-ENT FREQUENCIES

*Weichuan Zhao[1], Tianming Luo[1], Mohamad Ghaffarian Niasar[1]*

[1]*Technical University of Delft, Delft, the Netherlands*

**Keywords**: RAMP BREAKDOWN, EPOXY RESIN, IMMEDIATE TIME TO BREAKDOWN, PERMISSI-BLE ELECTRIC FIELD, HIGH FREQUENCY TRANSFORMER

## Abstract

In this study, the immediate time to breakdown for pure epoxy resin is measured by applying a ramp sinusoidal voltage signal at certain frequency (50Hz, 500Hz and 5000Hz) until breakdown occurs. The HV testing procedures, epoxy resin sample and experimental set-up preparation and Weibull analysis of obtained results are elaborated. The experiments were carried out on epoxy samples with the thickness between 0.1mm and 0.2mm and the thickness was divided into three groups for more accurate statistical analysis.

## 1 Introduction

The solid state transformer (SST) which could fulfill flexible voltage and power flow control is currently under development to be used in future power grid due to its excellent electrical performance. Besides, the reactive power compensation and large-scale sustainable energy integration could also be achieved by the application of SST [1]. Medium frequency transformer (MFT) which is expected to be used for galvanic isolation, voltage transformation and impedance matching [2] is the key component of SST. In fact, MFT could be regarded as an intermediate module connecting primary and secondary power electronic conversion circuits in SST.

The size of MFT is expected to be more compact to fit some electrical devices (i.e. high voltage arbitrary waveform generators). For reaching smaller size and higher energy transmission efficiency of MFT, the frequency level of MFT input voltage signal has increased significantly during the past two decades. Therefore, the study of high frequency insulation performance is necessary for the stable operation of dry-type MFT together with its ancillary power electronic equipments [1]. It is commonly known that the insulation material exposed to higher frequency ages faster. In [3], equation (1) which relates the material lifetime and frequency is proposed. For different insulation material, the value of n which determines the aging rate differs a lot.

$$L_f = L_1(\frac{f_1}{f})^n \qquad (1)$$

The material used for the built of insulation system of MFT must have outstanding insulating properties since the operating temperature can be high and the requirement of having small volume of MFT put limitation on the thickness of insulation system. Various types of insulation material

such as oil-paper insulation, epoxy resin, polyamide film, polypropylene and etc are potential candidates for the MFT insulation system.

With respect to the generation of MFT input signal, power electronic components (i.e. IGBT) were introduced to drive MFT. Due to fast-switching operation, harmonics, transients and ripples which could accelerate the degradation of MFT insulation system and cause the overheating problem are created. Thus, the material used for MFT insulation system ought to have sufficient high electrical endurance and thermal robustness. Moreover, the presence of partial discharges (PD) is also a potential threat for the reliability of the insulation. In many cases, PD is a major problem in high voltage (HV) insulation system and it can lead to the change of dielectric properties and ultimate failure of insulation materials [12].

Furthermore, electrical treeing is actually a pre-breakdown phenomenon in polymeric insulating material which occurs at the region of high divergent field such as the voids, grazes, protrusions, impurities and cracks [13]. Under high voltage applications, the excessive electrical field stress caused by defects would result in internal discharges within the small regions of dielectric and then form electrical treeing. Due to the limitation of material casting level, those mentioned defects are unavoidable. For the insulation with such defects, treeing and discharges are present and the breakdown probability and aging rate would be increased.

With respect to the selection of MFT insulation material, lifetime curve that reflects the material lifetime at certain field strength, temperature and frequency could provide valuable information. Based on such curves, proper thickness of insulation and sufficient electric field grading required for MFT design can be determined. However, in order to form lifetime curves, the figure which could indicate the insulation material breakdown strength range at different frequencies and tem-

peratures should be obtained first. Based on the breakdown strength curves, proper permissible field strength for aging tests could be decided. The selected field strength for aging tests should be around 10% higher than the minimum field stress. So far, the breakdown and lifetime for the insulation material under 50Hz have already been well-investigated in [1] and [4]. However, the research for insulation breakdown at higher frequency level are not adequate.

Epoxy resin is believed to be one of the most competitive insulation materials for MFT due to its excellent electrical, thermal and mechanical properties [5] and relatively smaller dissipation factor. These mentioned properties could also be significantly enhanced through adding certain amount of nano-fillers (i.e. hBN particles) [6-7]. In [12], N. Awang and his colleagues concluded that higher amount of BN nano-fillers results in a decrease in PD magnitude, the PD number and the PD charge as compared to the neat sample.

Moreover, the breakdown strength of pure epoxy resin is affected by various factors such as material thickness, slope of the applied AC voltage ramp, field stress duration, temperature, humidity and condition of dielectric (aged or brand-new) [9]. In order to obtain reasonable and convincing results, the slope of the ramp sinusoidal input voltage is set to be $1kV_p/s$. In this paper, the breakdown strength of pure epoxy resin is investigated and compared at 50Hz, 500Hz and 5000Hz at room temperature($20°C$).
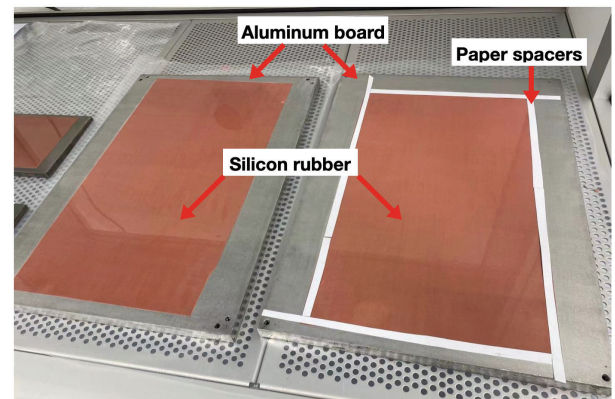
## 2 Epoxy sample preparation

In [10], Zhiqiang Xu and his colleagues have introduced a pre-made mould to create the thin epoxy resin samples. The spacers are placed within the mould to adjust the sample thickness. However, due to the large viscosity of epoxy resin, the removal of the sample from the mould after curing will be a big issue. Also, in [11], the authors provided the detailed interpretations for the preparation of the epoxy samples with the thickness of around 5mm.

In this study, epoxy resin type CY225 and hardener type HY925 supplied by the company Huntsman are the original materials used for sample preparation. To begin with, Teflon plates were used as the mould for samples because the cured epoxy wouldn't stick tightly on Teflon. However, after the curing process, Teflon material penetrated the epoxy resin sample and make it non-transparent. To reach more accurate results, Teflon-base mould was abandoned. If the epoxy resin material was poured in an open mould, the epoxy surface will be curved and shrined and thin samples cannot be made. It is worth mentioning that the pure epoxy needs hardener to create tightly cross-linked molecular structures that impart incredible strength into the cured film. Based on above information, the epoxy sample preparation processes with the thickness between 0.1mm and 0.2mm are shown as follow:

a) Epoxy resin (CY225) and hardener (HY925) were both degassed at $60°C$ for an hour in the chamber of BINDER VD 53 vacuum oven to remove air and moisture inside the original materials.

b) The degassed hardener (liquid-type) was added to epoxy resin and mixed thoroughly for around 30 minutes. Then, the mixture was placed inside BINDER VD 53 vacuum oven to remove the trapped air at $60°C$ for 2.5 hours.

c) Two large Aluminum plates were machined to fit the BINDER oven and used as the mould for epoxy resin sample casting and curing. For easier sample removal, a thin layer of silicon rubber with the thickness of 0.3mm was casted on the plates shown in fig. 1(a). (The silicon rubber layer is made by TFC Silicon Kautschuk TYP3-Basis and Catalyst, which was applied uniformly on the Aluminum plates by ZUA 2000 universal applicator.)

d) Paper spacers were placed at the edge of silicon rubber area shown in fig.1 and used to control the thickness of pure epoxy sample. The thickness for one layer of paper spacers is around 0.10mm. In order to acquire thicker samples, multiple layers of paper could be used. The degassed epoxy-hardener mixture was casted on the silicon rubber region and spread uniformly by ZUA 2000 universal applicator.

e) The epoxy resin sample was cured inside the oven type BINDER FD 53 at $120°C$ for four hours. Then, the sample was cooled down and cut into pieces for ramp breakdown tests. The thickness of the sample ranges from 0.08mm to 0.20mm shown in fig. 1(b).



*a*



b

2
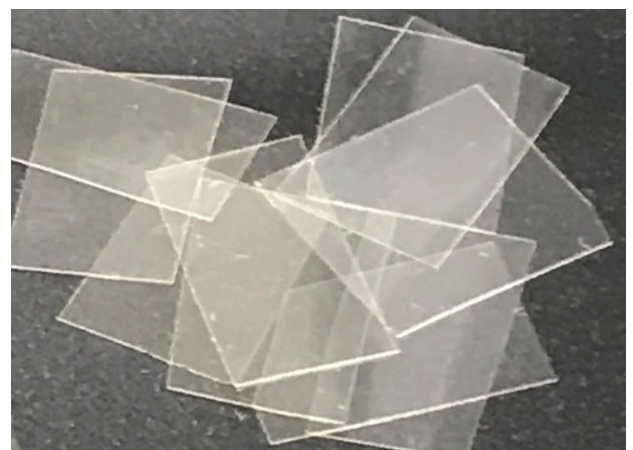
Fig. 1 (a) The pre-made mould for epoxy sample preparation (b) The thin epoxy resin sample pieces

## 3 Experimental set-up

The function generator type TENUMA 72-14111 is used to generate the input voltage signal with arbitrary frequencies. The sphere electrodes were immersed inside clean mineral oil to avoid the occurrence of surface discharges. In [18], John H. Mason has already proved that the surface discharge inception voltage in oil is much larger than that in air for similar thickness samples.

The magnitude of the input signal could be amplified by 3000 times through Trek amplifier which has the current limitation of 20mA and voltage limitation of 30kV. The Trek amplifier is equipped with an internal divider which is introduced to measure its output voltage.
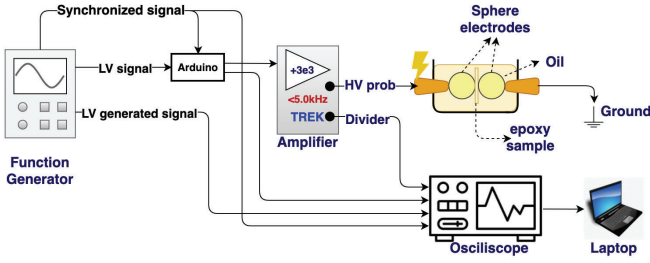


Fig. 2 Set-up for ramp breakdown and lifetime tests

In [2], [5] and [14-15], to create homogeneous electric field, double-sphere electrodes are used for AC ramp breakdown experiments. But in [3], cylinder electrodes are also implemented for the AC tests. Based on the information shown in [1] and [16], cylinder electrodes are indeed mainly used for DC breakdown tests. As a consequence, in this study, double-sphere electrodes made of brass with the diameter of 10mm are selected. The sketch of entire experimental setup is shown in fig. 2.

The Arduino, relay and some other accessories formed the control box of the set-up. The control box is connected between the function generator and Trek amplifier. The relay within the control box could only be turned on at the instant when the synchronization signal sent from function generator to Arduino dropped from high level to low level. Thus, the ramp voltage signal would definitely start at the very beginning and be sent to the Trek amplifier. In this way, all ramp breakdown tests were ensured to have same waveform start-point with an exact $1kV_p/s$ rate.

Moreover, relay within the control box could be deactivated when Arduino detects that the magnitude of voltage signal send from Trek amplifier internal divider is smaller than the determined minimal threshold $U_{min}$ for a pre-defined period of time. A fast fault detection is implemented and the amplifier input is turned off very quickly. As a result, the amount of discharge spots carbonized on the sphere electrodes would be reduced significantly and electrodes are only required to be polished and cleaned after each set of experiments.

## 4 Results for ramp breakdown tests

Ramp breakdown experiments were performed on thin epoxy samples with the thickness ranging from 0.1mm to 0.2 mm. A ramp sinusoidal voltage input signal with the slope of $1kV_p/s$ at 50Hz, 500Hz or 5000Hz was applied on one of the sphere electrodes. Moreover, the breakdown strength was measured through dividing the applied voltage to its relevant thickness nearby the breakdown perforation.

In [17], George Chen and his colleagues have mentioned that the electrical breakdown strength of solid dielectrics has been found to decrease with the increase in sample thickness and this type of phenomenon could be explained by the inverse power law shown as formula (2).

$$E(d) = k d^{-n} \tag{2}$$

With respect to formula (2), E represents for the breakdown strength of the insulation material at certain thickness. n and k are the two important constants that are associated with the testing material. This phenomenon could then be explained through volume effect. Sample with larger thickness would comprise of more defects (cavities, cracks) and the defects could induce discharges and reduce breakdown strength significantly.

In this study, the thickness of epoxy resin samples has been divided into three groups. Group one ranges from 0.105mm to 0.135mm (0.12±0.015mm). Group two and three range from 0.135mm to 0.165mm (0.15±0.0015mm) and from 0.165mm to 0.195mm (0.18±0.015mm) respectively. Fig. 3 illustrates an example of the variation of epoxy sample thickness used for 50Hz ramp breakdown tests.

2-parameter Weibull distribution analysis formula shown in (3) is used to analyze the data obtained from breakdown tests.

$$F(E) = 1 - e^{-(\frac{E}{\eta})^{\beta}} \tag{3}$$

In (3), E is breakdown strength and F(E) represents for the cumulative probability of breakdown. $\beta$ is shape parameter which reflects the slope of regressive line in the probability plot and $\eta$ represents for a certain breakdown strength whose failure rate is 63.2%. Furthermore, in Weibull distribution, there is another important parameter named correlation factor $\rho$, which is an indicator showing how well the linear regressive line fits the obtained data. Figure 4, 5 and 6 illustrate Weibull plots for breakdown strength of epoxy sample at those three thickness groups at 50Hz, 500Hz as well as 5000Hz separately. Moreover, Table 1-3 shows a summary of those mentioned Weibull distribution parameters for those corresponding figures.

Based on fig. 4, 5 and 6, it is rather obvious that the thinnest thickness group (blue dots) has considerably larger breakdown strength compared with that for the thicker groups (It could be verified through the comparison between parameter $\eta$ values shown in table I-III) due to the volume effect. Moreover, at higher frequency level, the surface discharges that could cause cumulative heating with higher repetition rate might also contribute to the reduction of sample breakdown

3

strength. According to fig. 4 and 6, it seems that the spread of ramp breakdown strength at 5kHz is relatively smaller than that at 50Hz. In order to properly fulfill the statistical analysis, for each thickness group, at certain frequency, at least 12 experiments were performed for the ramp sinusoidal breakdown tests.
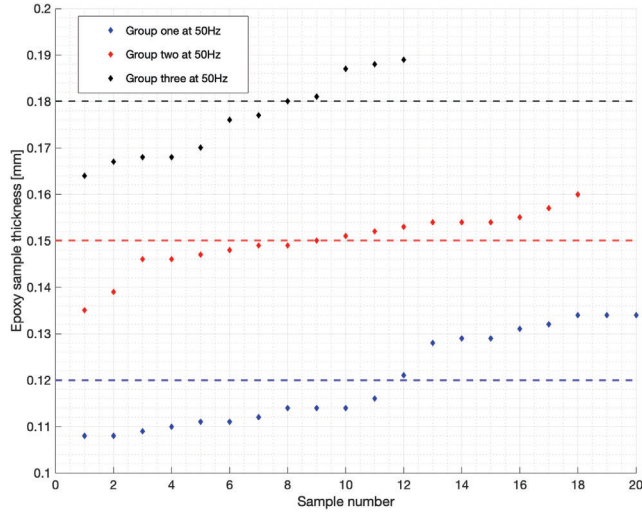


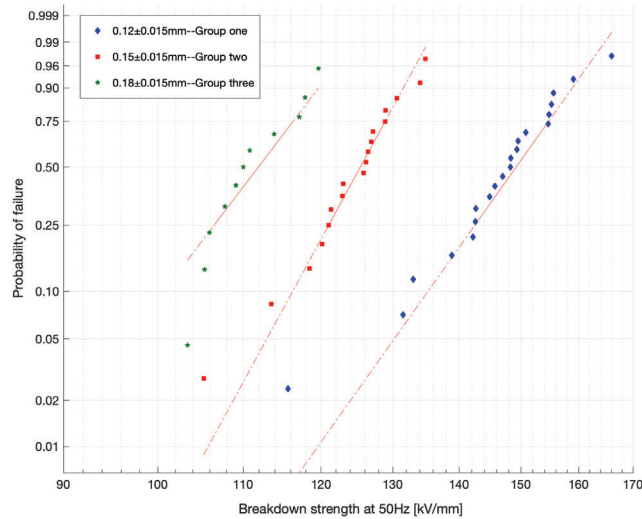Fig. 3 Variation of epoxy sample thickness used at 50Hz

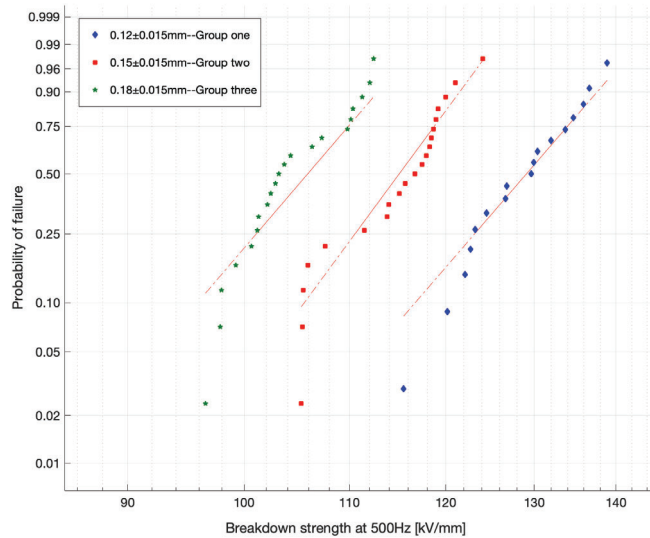

Fig. 4 Weibull plots for 3 thickness groups at 50Hz



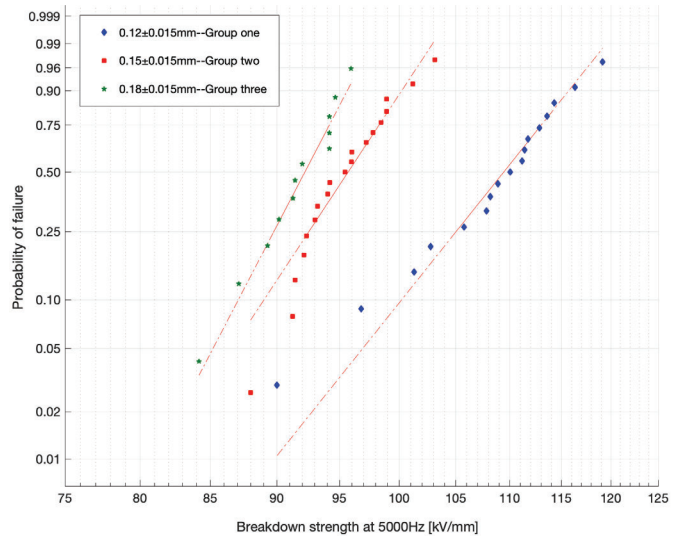Fig. 5 Weibull plots for 3 thickness groups at 500Hz



Fig. 6 Weibull plots for 3 thickness groups at 5000Hz

*4.1.1. Table I: Weibull distribution parameters for ramp breakdown results in different thickness ranges at **50 Hz***

| Parameter | $\beta$ | $\eta$ [kV/mm] | $\rho$ |
|---|---|---|---|
| Group one (thin) | 16.05 | 151.17 | 0.980 |
| Group two (middle) | 22.49 | 127.23 | 0.986 |
| Group three (thick) | 22.68 | 113.54 | 0.949 |

In reality, the important Weibull parameters placed in Table I-III were all calculated based on formula (3). From the calculation, what could be obtained is a narrow range of $\eta$ and $\beta$ values. (For instance, at 50Hz, the range of $\beta$ from group one is 16.05±0.75 and the average value 16.05 was chosen.) In order to reduce the range, more experiments should be performed. Based on the values shown in Table I-III, it seems that the slope of regressive line for Group one is smaller than that for Group two and Group three. The slope for Group two and three are more or less similar. Also, for each frequency level, it seems that the regressive line slope has a trend to increase with the increase of the sample thickness. This could be verified through more experiments on each certain case, which is also our future planning work.

*4.1.2 Table II: Weibull distribution parameters for ramp breakdown results in different thickness ranges at **500 Hz***

| Parameter | $\beta$ | $\eta$ [kV/mm] | $\rho$ |
|---|---|---|---|
| Group one (thin) | 24.00 | 131.38 | 0.986 |
| Group two (middle) | 25.13 | 117.28 | 0.953 |
| Group three (thick) | 26.99 | 106.55 | 0.945 |

4

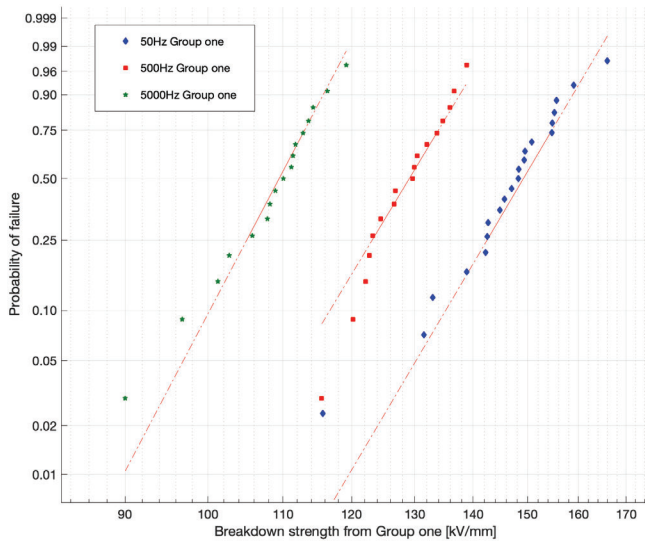| Parameter | $\beta$ | $\eta$ [kV/mm] | $\rho$ |
|---|---|---|---|
| Group one (thin) | 17.39 | 111.72 | 0.990 |
| Group two (middle) | 31.57 | 97.07 | 0.967 |
| Group three (thick) | 33.67 | 93.03 | 0.990 |



Fig. 7 Weibull plots in the thickness Group one (thin)

Based on fig. 7-9, it is clear that at each thickness group, the ramp breakdown strength obtained at lower frequency (i.e 50Hz) is much larger than that obtained at higher frequency (i.e 5000Hz), which could also be regarded as a proof that higher frequency signal ages insulation material faster (This could also be verified by the comparison of the Weibull parameter $\eta$ in Table I-III).
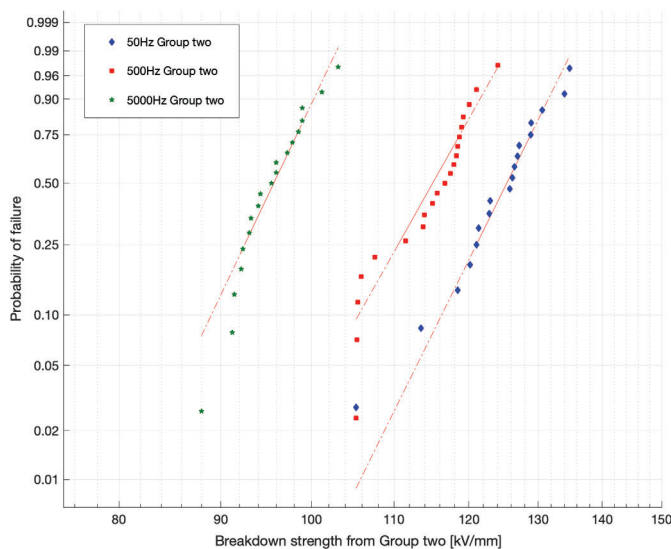


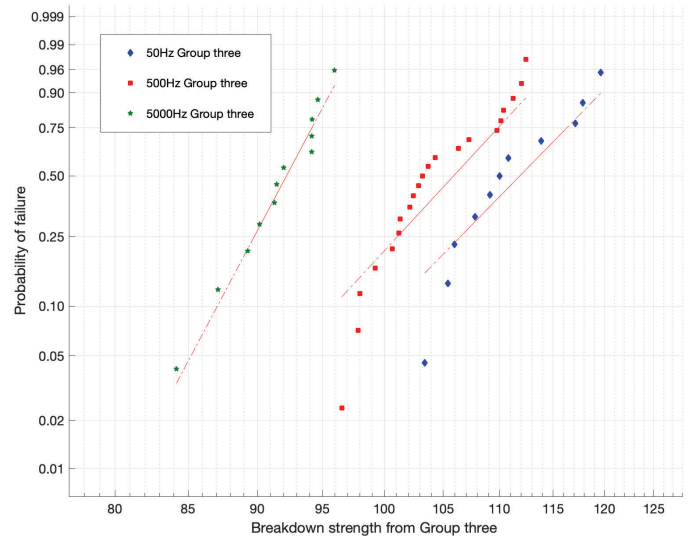Fig. 8 Weibull plots in thickness Group two (middle)



Fig. 9 Weibull plots in thickness Group three (thick)

It is commonly known that breakdown is more likely to happen at the peak of waveform because at that point both voltage and field strength reach to the maximum. Moreover, it is also observable through the experiments that breakdown could happen at both polarities (negative and positive), most of the breakdown cases take place close to the peak or at the peak and some happen off the peak. Fig. 10-11 illustrate two examples acquired from oscilloscope of such breakdown that happen off the peak.



a



5
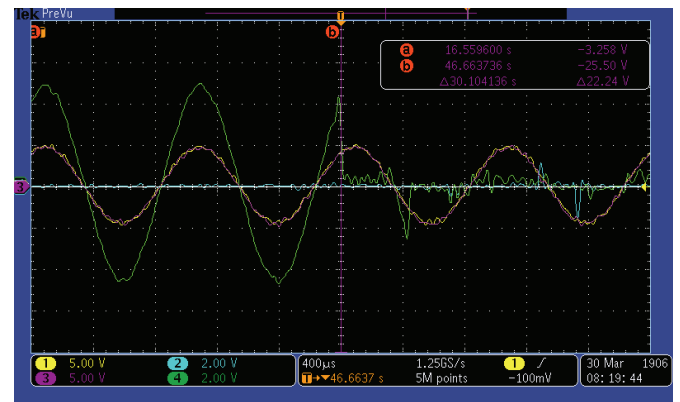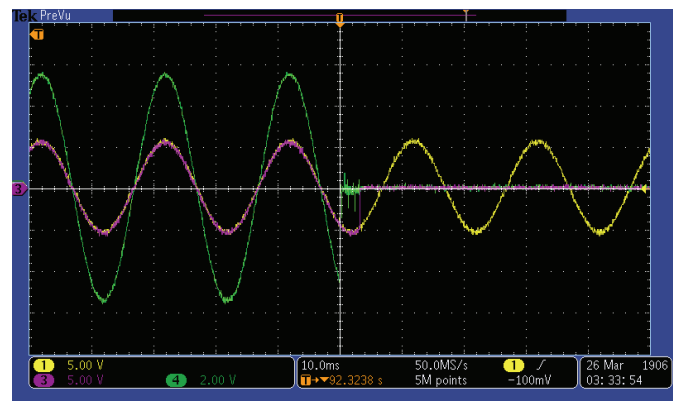
b

Fig.10 (a) Breakdown off the peak at 50Hz in negative part (b) Breakdown off the peak at 500Hz in positive part

## 5    Conclusion

In this study, breakdown strength of thin epoxy resin samples were investigated at 50Hz, 500Hz and 5kHz. For the ramp breakdown tests, it could be summarized that the breakdown strength of pure epoxy is really sensitive to the thickness. The breakdown strength is much larger for thinner sample compared with that for thicker sample. Also, for the same thickness level, the breakdown strength for higher frequency is much smaller than that for lower frequency.

## 6    Acknowledgements

## 7    References

[1] Y. Zhao, G. Zhang, D. Han, et al. "Experimental study on the insulation properties of epoxy casting resins under high-frequency square waveform." CSEE Journal of Power and Energy Systems, doi: 10.17775/CSEEJPES.2019.02110.

[2] X. Wang, W. Wang, Y. Liu, et al. "Influence of High Frequency Voltage with Harmonic Contents and Temperature on Breakdown of Epoxy Resin Used in Power Electronic Transformer." 2020 International Symposium on Electrical Insulating Materials (ISEIM), 2020, pp. 462-465.

[3] D. Fabiani, G. C. Montanari, A. Cavallini, et al. "Relation between space charge accumulation and partial discharge activity in enameled wires under PWM-like voltage waveforms." IEEE Transactions on Dielectrics and Electrical Insulation, vol. 11, no. 3, pp. 393-405, June 2004, doi: 10.1109/TDEI.2004.1306718.

[4] J. Wu, H. Jin, A. R. Mor, et al. "The effect of frequency on the dielectric breakdown of insulation materials in HV cable systems." 2017 International Symposium on Electrical Insulating Materials (ISEIM), 2017, pp. 251-254, doi: 10.23919/ISEIM.2017.8088734.

[5] Z. Xing et al., "Study on DC breakdown characteristics of epoxy insulating materials." 2018 12th International Conference on the Properties and Applications of Dielectric Materials (ICPADM), 2018, pp. 1119-1122, doi: 10.1109/ICPADM.2018.8401242.

[6] Y. Murakami, T. Matsubara, T. Kawashima, et al. "Basic electrical characteristics of epoxy/hollow silica composites influenced by addition of hollow silica." 2019 Electronics and communications in Japan, pages 387-392.

[7] H. Jin, I. Tsekmes, J. Wu, et al. "The effect of frequency on the dielectric strength of epoxy resin and epoxy resin based nanocomposites." 2017 International Symposium on

Electrical Insulating Materials (ISEIM), 2017, pp. 141-143, doi: 10.23919/ISEIM.2017.8088708.

[8] L. desmars, J. galy, D. bachellerie, et al. "High Voltage Electrical Properties of Epoxy / h-BN Microcomposites." 2018 IEEE 2nd International Conference on Dielectrics (ICD), 2018, pp. 1-5, doi: 10.1109/ICD.2018.8514777.

[9] H. Yahyaoui, P. Notingher, S. Agnel, et al. "Electrical breakdown of epoxy and PTFE under dc conditions." 2016 IEEE International Conference on Dielectrics (ICD), 2016, pp. 1-4, doi: 10.1109/ICD.2016.7547526.

[10] M. Reading, Z. Xu, A. S. Vaughan, et al. "The thermal and electrical properties of nano-silicon dioxide filled epoxy systems for use in high voltage insulation." 2011 Electrical Insulation Conference (EIC)., 2011, pp. 493-497, doi: 10.1109/EIC.2011.5996206.

[11] H. Fu, C. Zhang, J. Xiang, et al. "Electrical Tree Characteristics of Epoxy Resin under Bipolar Square Wave Voltage." 2020 IEEE 3rd International Conference on Dielectrics (ICD), 2020, pp. 142-145, doi: 10.1109/ICD46958.2020.9341976.

[12] N. Awang, et al. "Experimental investigation on partial discharge characteristics of epoxy-nanocomposite as high voltage insulation material." 2014 IEEE International Conference on Power and Energy (PECon), 2014, pp. 146-149, doi: 10.1109/PECON.2014.7062430.

[13] M. H. Ahmad, et al. "Effects of oil palm empty fruit bunch filler on electrical tree propagation in Epoxy resin." 2012 International Conference on High Voltage Engineering and Application, 2012, pp. 203-206, doi: 10.1109/ICHVE.2012.6357076.

[14] S. Harada, M. Kozako, M. Hikita, et al. "Preparation of fullerene/epoxy resin composite with fine dispersion and its breakdown strength." 2017 International Symposium on Electrical Insulating Materials (ISEIM), 2017, pp. 654-656, doi: 10.23919/ISEIM.2017.8166575.

[15] I. A. Tsekmes, R. Kochetov, P. H. F. Morshuis, et al. "AC breakdown strength of epoxy-boron nitride nanocomposites: Trend & reproducibility." 2015 IEEE Electrical Insulation Conference (EIC), 2015, pp. 446-449, doi: 10.1109/ICACACT.2014.7223609.

[16] I. A.Tsekmes, R. Kochetov, P. H. F. Morshuis, et al. "DC breakdown strength of epoxy-boron nitride nanocomposites: Trend and reproducibility." 2015 IEEE Conference on Electrical Insulation and Dielectric Phenomena (CEIDP), 2015, pp. 479-482, doi: 10.1109/CEIDP.2015.7352014.

[17] G. Chen, J. Zhao, S. Li, et al. "Origin of thickness dependent dc electrical breakdown in dielectrics." Applied Physics Letters. 100. 10.1063/1.4721809.

[18] John H. Mason. "Effects of frequency on electric stress on Polymers." IEEE Transactions on Electrical Insulation. Vol.27, No.6, December 1992.

6